An Optimal Robust Digital Image Watermarking Based on Genetic Algorithms in Multiwavelet Domain

PRAYOTH KUMSAWAT[1], KITTI ATTAKITMONGCOL[2] AND ARTHIT SRIKAEW[2]
[1]School of Telecommunication Engineering, [2]School of Electrical Engineering
Institute of Engineering, Suranaree University of Technology
111 University Avenue, Muang District, Nakhon Ratchasima, 30000, THAILAND
E-mail: {prayoth, kitti, ra}@sut.ac.th

Abstract:- In this paper, we propose digital image watermarking algorithm in the multiwavelet transform domain. The embedding technique is based on the quantization index modulation technique and this technique does not require the original image in the watermark extraction. We have developed an optimization technique using the genetic algorithms to search for optimal quantization steps to improve the quality of watermarked image and robustness of the watermark. In addition, we analyze the performance of the proposed algorithm in terms of peak signal to noise ratio and normalized correlation. The experimental results show that our proposed method can improve the quality of the watermarked image and give more robustness of the watermark as compared to previous works.

Key-Words: - Image watermarking; Multiwavelet; Multiwavelet tree; GA; Quantization index modulation

1 Introduction

In recent years, digital multimedia technology and communication network have made great progress. Various kinds of multimedia content have been widely distributed through the Internet. Consequently, intellectual property protection is a pressing concern for content owners who are exhibiting digital representation of the photographs, music, video and original artworks through the Internet.

Digital watermarking is one of the most popular approaches considered as a tool for providing the copyright protection of digital contents. This technique is based on direct embedding of additional information data into the host signal for identifying the copyright ownership. There are many digital watermarking techniques reported in the literature. For digital images, the embedding process can be accomplished in either spatial domain or transform domain. However, watermarking techniques based on transform domain are more popular than those based on spatial domain since they provide higher image quality and much more robust watermark [1].

According to the need of original data during watermark detection process, watermarking algorithms are classified into private algorithm and public or blind one. Private method needs the original signal during detection. In some cases, when the original data is not easy to obtain, or when we do not know which copy is the original one, it is necessary to used blind watermarking for resolving rightful ownership.

In [2], Chen and Wornell proposed a class of embedding methods called quantization index modulation (QIM) that achieves probably good rate-distortion-robustness performance. Wu *et al.* [3] proposed a self-synchronization algorithm for audio watermarking using QIM method. They embed the synchronization codes with hidden informative data so that the hidden data has self-synchronization ability. Synchronization codes and informative bits are embedded into low-frequency subband in wavelet domain. Their simulations suggest that the quantization step greatly depends on types and magnitudes of the original audio signals. It is not the best choice to use a fixed quantization step. Xiong *et al.* [4] proposed a multipurpose image watermarking method based on adaptive quantization of wavelet coefficients. The selection of quantization steps is related to the functions of sub-watermarks and adaptive to the texture feature of image. Wang and Lin [5] proposed a wavelet tree quantization for copyright protection watermarking. The wavelet coefficients are grouped into a predefined structure called supertree. Watermark bits are also embedded by quantizing supertree and the resulting difference between quantized and unquantized trees will later be used for watermark extraction.

In recent years, some multiwavelet-based digital watermarking algorithms have been proposed. Ghouti *et al.* [6] introduced a robust watermarking

algorithm using balanced multiwavelet transform. The watermark embedding scheme is based on the principles of spread-spectrum communications to achieve higher watermark robustness. In [7, 8], Kumsawat *et al.* proposed a new digital image watermarking algorithm in the multiwavelet transform domain. The embedding technique is based on the parent-child structure of the transform coefficient called the triple tree. The watermark is a binary pseudo-random noise sequence and does not require the original image in the watermark extraction.

Improvements in performance of image watermarking schemes can be obtained by exploiting the characteristics of the human visual system (HVS) in watermarking process. It is possible to embed perceptually invisible watermarks with high energy in an image, which makes watermark very robust [1, 2, 9]. Another way to improve the performance of watermarking schemes is to make use of artificial intelligence techniques. The image watermarking problem can be viewed as an optimization problem. Therefore, it can be solved by optimization algorithm such as genetic algorithms (GA), adaptive tabu search (ATS), support vector machine (SVM) or neural network (NN). There has been a few research in application of GA to image watermarking problems. In [10], Huang *et al.* proposed a watermarking method based on the discrete cosine transform (DCT) and genetic algorithm. They embed the watermark with visually recognizable patterns into the image by selectively modifying the middle-frequency parts of the image. The GA is applied to search for the locations to embed the watermark in the DCT coefficient block such that the quality of the watermarked image is optimized. In [11], Shieh *et al.* proposed a robust image watermarking in DCT domain. They make use of GA to find the optimal frequency bands for watermark embedding into the DCT-based watermarking system, which can simultaneously improve security, robustness, and image quality of the watermarked image. Kumsawat *et al.* [12] proposed the spread spectrum image watermarking algorithm using the discrete multiwavelet transform (DMT). The GA is applied to search for optimal watermarking parameters to improve the quality of the watermarked image and the robustness of the watermark. In [13], Shih and Wu proposed a novel technique in correcting the rounding errors for both robust and fragile watermarks. They employ genetic algorithm to find

the suitable solution in translating the real numbers into integers during the discrete cosine transformation. Zhong *et al.* [14] presented a watermarking optimization technique in the wavelet transform domain. They make use of GA to search for parameters which consist of time of Arnold transform and the embedding strength to improve the visual quality of watermarked images and the robustness of the watermark. In [15], Sriyingyong and Attakitmongcol proposed a robust audio watermarking method based on the DWT and the adaptive tabu search. ATS is applied to search for optimal intensity of watermark such that the watermarked audio quality is optimized. Wang *et al.* [16] proposed an image watermarking scheme in spatial domain and applied classification techniques based on SVM to improve the performance of conventional methods. In [17], Zhang proposed a new blind watermarking scheme based on discrete wavelet transform and neural networks. Due to the learning and adaptive capabilities of the radial basis function in neural networks, the embedding and extracting strategies can greatly improve the robustness against various attacks.

In this paper, we propose an image watermarking method based on the discrete multiwavelet transform for the application of copyright protection. In our algorithm, the watermark is embedded into the multiwavelet triple tree using QIM technique. The imperceptibility and robustness of an existing image watermarking technique is enhanced through GA optimization. The proposed watermarking technique is resistant against various image processing attacks as will be demonstrated in the examples. Finally, we have compared our experimental results with the results of previous work.

This paper is organized as follows: in Section 2, the preliminaries of multiwavelet transform, multiwavelet tree and genetic algorithm are introduced. Watermarking in the DMT domain with genetic algorithm optimization is described in Section 3. In Section 4, the experimental results are shown. The conclusions of our study can be found in Section 5.

2 Preliminaries

2.1 Multiwavelet Transform

Multiwavelet transform is a relatively new concept in the framework of wavelet transform and has

some important differences. In particular, whereas wavelet has a one scaling function and wavelet function, multiwavelet has two or more scaling and wavelet functions. The main motivation of using multiwavelet is that it is possible to construct multiwavelets that simultaneously possess desirable properties such as orthogonality, symmetry and compact support with a given approximation order [18]. These properties are not possible in any scalar wavelet. A brief overview of the multiwavelet transform is described next.

Let Φ denote a compactly supported orthogonal scaling vector $\Phi = (\phi^1, \phi^2, ..., \phi^r)^T$ where r is the number of scalar scaling functions. Then $\Phi(t)$ is satisfy a two-scale dilation equation of the form

$$\Phi(t) = \sqrt{2} \sum_n h(n) \Phi(2t - n) \qquad (1)$$

for some finite sequence h of $r \times r$ matrices. Furthermore, the integer shifts of the components of Φ form an orthonormal system, that is

$$<\phi^l(\cdot - n), \phi^{l'}(\cdot - n')> = \delta_{l,l'} \delta_{n,n'}. \qquad (2)$$

Let V_0 denote the closed span of $\{\phi^l(\cdot - n) \mid n \in Z, l = 1, 2, ..., r\}$ and define $V_j = \{f(\frac{\cdot}{2^j}) \mid f \in V_0\}$. Then $(V_j)_{j \in Z}$ is a multiresolution analysis of $L^2(R)$. Note that we choose the decreasing convention $V_{j+1} \subset V_j$.

Let W_j denote the orthogonal complement of V_j in V_{j-1} Then there exists an orthogonal multiwavelet $\Psi = (\psi^1, \psi^2, ..., \psi^r)^T$ such that $\{\psi^l(\cdot - n) \mid l = 1, 2, ..., r$ and $n \in Z\}$ form an orthonormal basis of W_0. Since $W_0 \subset V_{-1}$, there exists a sequence g of $r \times r$ matrices such that

$$\Psi(t) = \sqrt{2} \sum_n g(n) \Phi(2t - n). \qquad (3)$$

Let $f \in V_0$, then f can be written as a linear combination of the basis in V_0:

$$f(t) = \sum_n c_0(k)^T \Phi(t - k) \qquad (4)$$

for some sequence $c_0 \in l_2(Z)^r$. Since $V_0 = V_1 \oplus W_1$, f can also be expressed as

$$f(t) = \frac{1}{\sqrt{2}} \sum_{k \in Z} c_1(k)^T \Phi(\frac{t}{2} - k)$$
$$+ \frac{1}{\sqrt{2}} \sum_{k \in Z} d_1(k)^T \psi(\frac{t}{2} - k). \qquad (5)$$

The coefficients c_1 and d_1 are related to c_0 via the following decomposition and reconstruction algorithm:

$$c_1(k) = \sum_n h(n) c_0(2k + n) \qquad (6)$$

$$d_1(k) = \sum_n g(n) c_0(2k + n) \qquad (7)$$

$$c_0(k) = \sum_n h(k - 2n)^T c_1(n)$$
$$+ \sum_n g(k - 2n)^T d_1(n). \qquad (8)$$

Unlike scalar wavelet, even though the multiwavelet is designed to have approximation order p, the filter bank associated with the multiwavelet basis does not inherit this property. Thus, in applications, one must associate a given discrete signal into a sequence of length $-r$ vectors without losing some certain properties of the underlying multiwavelet. Such a process is referred to as prefiltering. The block diagram of a multiwavelet with prefilter $Q(z)$ and postfilter $P(z)$ is shown in Fig. 1. $H(z)$ and $G(z)$ are the z transform of $h(n)$ and $g(n)$, respectively. Figure 2(a) illustrates a single-level multiwavelet decomposition of the Lena image using the DGHM multiwavelet with optimal orthogonal prefilter [19], while the subband arrangement is illustrated in Fig. 2(b). The three detail subbands are denoted by LH (vertical orientation), HL (horizontal orientation) and HH (diagonal orientation), whereas the approximation subband is denoted by LL.
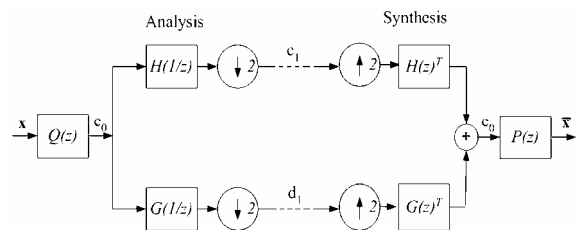

Fig. 1 Multiwavelet filter bank

2.2 Multiwavelet Tree

Multiwavelet transform coefficients have the property that the related coefficients in different scales are located at the same orientation and location in the multiwavelet hierarchical decomposition. Figure 3(a) illustrates a four-level multiwavelet decomposition of the Lena image.

With the exception of the highest frequency subbands, every coefficient at a given scale can be related to a set of coefficients at the next finer scale of similar orientation. The coefficient at the coarse scale is called the parent, and all coefficients corresponding to the same spatial location at the next finer scale of similar orientation are called children. For the four-level multiwavelet hierarchical subband decomposition, the parent-child dependencies are shown in Fig. 3(b). For a given parent, the set of all coefficients at all finer scales of similar orientation corresponding to the same location are called descendants. A multiwavelet tree descending from a single coefficient in the subband HL_4 is shown in Fig. 3(b).
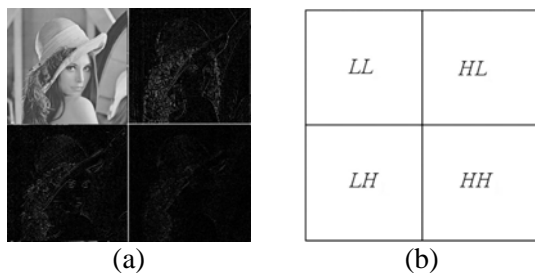

(a)   (b)

Fig. 2 (a) One-level multiwavelet decomposition of Lena image having size of 512×512 pixels and (b) the subband arrangement.
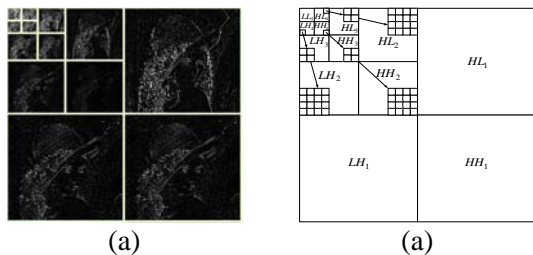

(a)   (a)

Fig.3 (a) Four-level multiwavelet decomposition of Lena image and (b) the parent-child dependencies of multiwavelet tree.

Without significant loss of generality, we shall focus on watermarking still images with 256 gray levels of size 512×512 pixels. To trade off between the invisibility and robustness of the watermark, the high-energy subband (LL_4) is not used. Furthermore, the coefficients in high-frequency subbands (LH_1, HL_1 and HH_1) are not used since they often contain low energy coefficients.
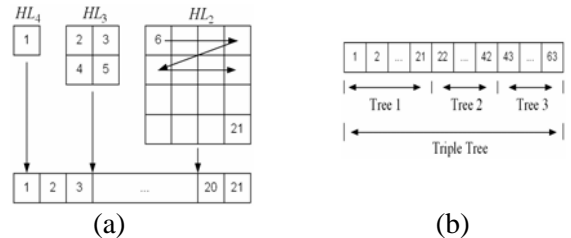

(a)   (b)

Fig.4 (a) A group of multiwavelet coefficients in each tree and (b) the example of triple tree

In other subbands, we group the coefficients corresponding to the same spatial location together. Figure 4(a) shows an example of a group with one coefficient from HL_4, 4 coefficients from HL_3, and 16 coefficients from HL_2. The coefficients of the same group correspond to various frequency bands of the same spatial location and the same orientation. The total number of groups is equal to the sum of the number of coefficient in LH_4, HL_4 and HH_4, each of which has 32×32 coefficients. There are a total of $3 \times 32 \times 32 = 3072$ groups. We denote each group of multiwavelet tree by Tg_m, where $m = 1, 2, ..., 3072$.

2.3 Genetic Algorithms

Genetic algorithms (GA) [20] are one of the most widely used artificial intelligent techniques for optimization. A GA is a stochastic searching algorithm based on the mechanisms of natural selection and genetics. GA have been proven to be very efficient and stable in searching for global optimum solutions. Usually, a simple GA is mainly composed of three operations: selection, genetic operation and replacement. A brief summary for implementing GA can be summarized as follows:

Defining the solution representation of the system is the first task of applying GA. GA use a population, which is composed of a group of chromosomes, to represent the solutions of the system. The solution in the problem domain can then be encoded into the chromosome in the GA domain and vice versa. Initially, a population is randomly generated. The fitness function then uses objective values from objective function to evaluate the fitness of each chromosome. The fitter

chromosome has the greater chance to survive during the evolution process. The objective function is problem-specific; its objective value can represent the system performance index (e.g. an error). Next, a particular group of chromosomes is chosen from the population to be parents. The offspring is then generated from these parents by using genetic operations, which normally are crossover and mutation. Similar to their parents, the fitness of the offspring is evaluated and used in replacement processes in order to replace the chromosomes in the current population by the selected offspring. The GA cycle is then repeated until a desired termination criterion is satisfied, for example, the maximum number of generations is reached or the objective value is below the threshold. There are various techniques in designing GA that we have to take into account. These include encoding schemes, fitness evaluation, parent selection, genetic operations and replacement strategies.

3 Proposed Method

In this section, we first give a brief overview of the watermark embedding and watermark extracting processes in the DMT domain. We then describe the GA optimization of our proposed method.

3.1 Watermark Embedding Algorithm

The watermark embedding algorithm is described as follows:

1. Generate a seed by mapping a signature or text through a one-way deterministic function. The seed is used as the secret key (K) for watermarking.

2. Generate a random watermark W using the secret key, where W is a binary pseudo-random noise sequence of watermark bits, and $W = \{w_i\}$ for $i = 1, 2,..., N_w$, where N_w is the length of watermark and $w_i \in \{+1, -1\}$.

3. Transform the original image into four-level decomposition using the DMT. Then, create multiwavelet trees and rearrange them into 3072 groups.

4. To increase the watermarking security, we order the groups Tg_m in a pseudorandom manner. The random numbers can be generated using the secret key K. We further combine the coefficients of every three groups together to form "a triple tree: Tt_i", for $i = 1, 2,..., 1024$. Each watermark bit is embedded into one triple tree. An example of a triple tree is shown in Fig. 4(b).

5. For watermark embedding, we select the first N_w triple trees, which have the largest mean values. Then, the watermark sequence $\{w_i\}$ is embedded into the selected triple trees by quantization index modulation technique. The quantization function is given as follows:

$$Tt_i' = \begin{cases} \lfloor Tt_i / S_j \rfloor \cdot S_j + 3S_j / 4 & if \ w_i = +1 \\ \lfloor Tt_i / S_j \rfloor \cdot S_j + S_j / 4 & if \ w_i = -1 \end{cases} \quad (9)$$

, where $\lfloor x \rfloor$ rounds to the greatest integer smaller than x, Tt_i and Tt_i' denote the triple tree of the original image and the corresponding watermarked image respectively. The variable S_j, for $j = 1, 2, 3$, denotes the quantization steps corresponding to the orientation of horizontal, vertical and diagonal of DMT subband, respectively. A large S_j makes the watermark robust, but it will destroy the original quality of the image. Thus, the value of S_j should be as large as possible under the constraint of imperceptibility.

6. In order to improve both quality of watermarked image and robustness of the watermark, this work employs the genetic algorithm to search for the quantization steps. The details of GA optimization process will be described in details in Section 3.3.

7. Pass the modified DMT coefficients through the inverse DMT to obtain the watermarked image. The watermark embedding process is shown in Fig. 5.
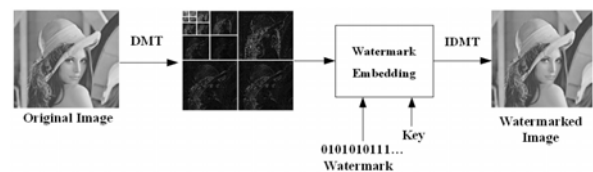

Fig. 5 Watermark embedding process

3.2 Watermark Extracting Algorithm

The watermark extracting algorithm is outlined as follows:

1. Transform the watermarked image into four-level decomposition using the DMT. Then, create the multiwavelet trees and rearrange them into 3072 groups.

2. We order the groups in a pseudorandom manner by a similar secret key which was used in the embedding process. Then, combine every 3 groups to form a triple tree Tt_n, for $n = 1, 2,..., 1024$.

3. Let $\tilde{T}t_i$ denote the first N_w triple trees, which have the largest mean values. The embedded watermark can be extracted from $\tilde{T}t_i$ by using the following rule:

$$\tilde{w}_i = \begin{cases} +1 & if \quad \tilde{T}t_i - \lfloor \tilde{T}t_i / S_j \rfloor \cdot S_j \geq S_j / 2 \\ -1 & if \quad \tilde{T}t_i - \lfloor \tilde{T}t_i / S_j \rfloor \cdot S_j < S_j / 2 \end{cases} \quad (10)$$

4. After extracting the watermark, we used normalized correlation coefficients to quantify the correlation between the original watermark and the extracted one. A normalized correlation (NC) between W and $\tilde{W}$ is defined as:

$$NC(W,\tilde{W}) = \frac{\sum_{i=1}^{N_w} w_i \tilde{w}_i}{\sqrt{\sum_{i=1}^{N_w} w_i^2 \sum_i \tilde{w}_i^2}} \quad (11)$$

, where W and $\tilde{W}$ denote an original watermark and extracted one, respectively and $\tilde{W} = \{\tilde{w}_i\}$ for $i = 1, 2,..., N_w$. The watermark extracting process is shown in Fig. 6.
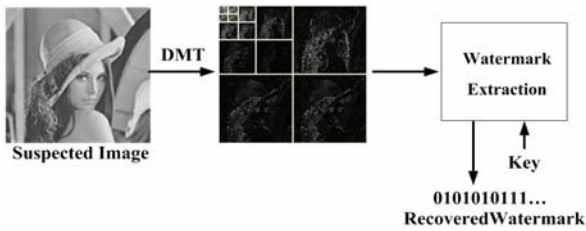

Fig. 6 Watermark extracting process

3.3 Genetic Algorithms Optimization

Recently, the idea of using a robust digital watermark to detect and trace copyright violations has motivated significant interest among publishers and content owners. The goals of an effective watermarking, such as imperceptibility, robustness and data capacity are usually conflicting [10, 11, 12]. In order to minimize such conflicts, this work employs the genetic algorithms to search for optimal parameters. This allows the system to achieve optimum performance for digital image watermarking.

For the optimization process, GA is applied in the watermark embedding and the watermark extracting processes. The parameters to be searched for are three quantization steps S_1, S_2 and S_3. The objective function of searching process is computed using factors that both related to robustness and imperceptibility of watermarked image. A high quality output image and robust watermark can then be achieved. The diagram of our proposed algorithm is shown in Fig. 7. Details of GA are described as follows:
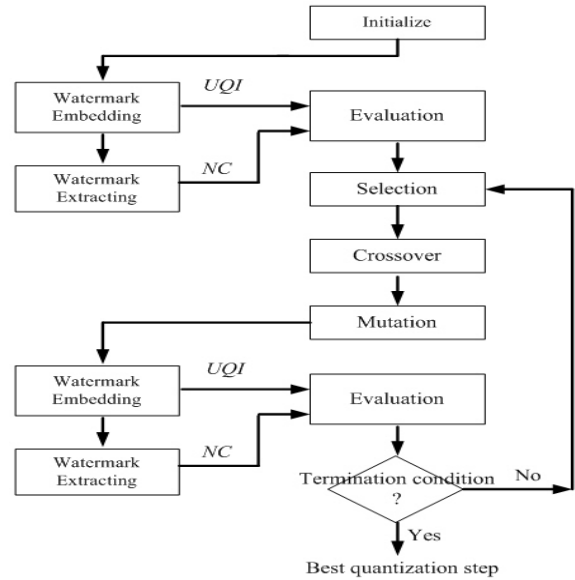

Fig. 7 Optimization diagram for digital image watermarking using genetic algorithms

Chromosomes in GA represent desired parameters to be searched. Number of chromosomes used in this work is 30. The encoding scheme is binary string with 32 bit resolutions for each chromosome. The parameter S_j is then represented by chromosome with length of 96 bits. The objective function uses both a universal quality index (UQI) [21] and normalized correlation as performance indices. UQI is used as output image quality performance index due to its role of imperceptibility measure. Similarly, NC is used as a watermark detection performance index because of its role of robustness measure. An objective value W can be calculated from equation (12):

$$W = \delta_{UQI} \times UQI + \delta_{NC} \times NC \quad (12)$$

, where δ_{UQI} and δ_{NC} are weighting factors of UQI and NC, respectively. These weighting factors represent the significance of each index used in GA searching process. If both indices are equally significant, the values of these factors will be 0.5 each where the relationship $\delta_{UQI} + \delta_{NC} = 1.0$ must

always hold. By using objective function W above, the parameter S_j can be optimally searched to achieve the best of both output image quality and watermark robustness. In this work, a ranking selection is chosen for selection mechanism. The crossover and mutation probability is fixed at 0.7 and 0.05, respectively. The chromosomes are then partially replaced by the best chromosome for each generation. The GA process is repeated until the most fit chromosome, i.e. parameter S_j, is optimally found.

4 Experimental Results and Discussions

To evaluate the performance of the proposed watermarking scheme, experiments have been conducted in which a DGHM multiwavelet was used to decompose the original image. The original image is a 256 gray-level image with the size of 512×512 pixels and the watermark length $N_w = 512$. Figures 8–12 show the convergence of GA optimization at 30 generations of the 4 test images: Lena, Baboon, Goldhill and Peppers. The results of optimal parameters S_1, S_2 and S_3 from GA searching using several test images with different characteristics are shown in Table 1. These parameters are optimally varied to achieve the most desirable ones for original image with different characteristics.

We test the output image quality by watermarking the original images with the resulting parameters from GA. Then, we measured the quality of the watermarked image by using the peak signal to noise ratio ($PSNR$). The PSNR values of the watermarked images are also shown in Table 1. Figures 13–14 show the original and watermarked version of the Lena image using the proposed technique, respectively. It can be seen that the watermarked image is not perceptually different from the original one. We also measured the normalized correlation of the untouched watermarked image. From Table 1, the $PSNR$ and NC values for all the tested images are about 46 dB and 1, respectively.

The watermarked images are attacked by various image compression and manipulations. Then, we perform the watermark extraction process and compute the normalized correlation. The results obtained from our proposed method which is called DMTGA are compared with the method based on wavelet-tree quantization in [5] and the

method based on multiwavelet tree in [8]. The $PSNR$ of the watermarked images and watermark length of both methods are about 38 dB and 512 bits, respectively. The comparison results are listed in Table 2 to Table 10.

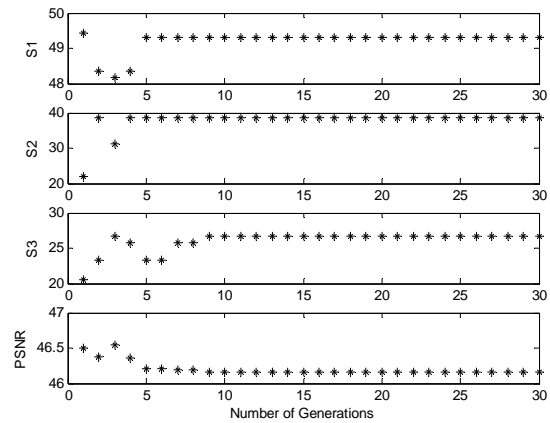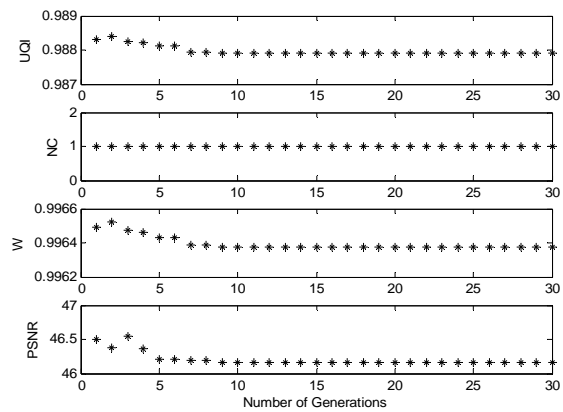Fig.8 S_1, S_2, S_3 and $PSNR$ from GA optimization process of the Lena image

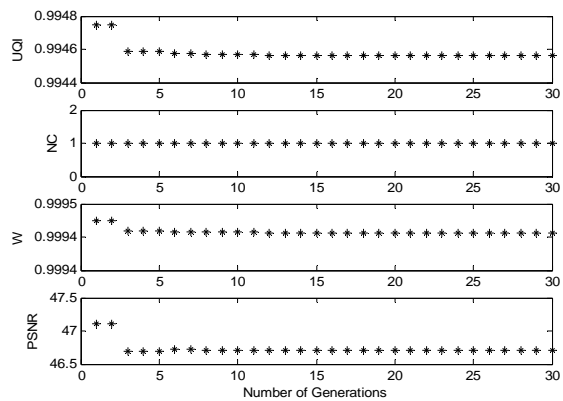Fig.9 UQI, NC, W and $PSNR$ from GA optimization process of the Lena image

Fig.10 UQI, NC, W and $PSNR$ from GA optimization process of the Baboon image
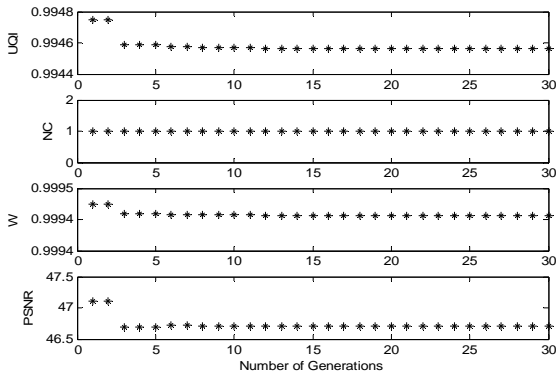
Fig.11 UQI , NC , W and $PSNR$ from GA optimization process of the Goldhill image
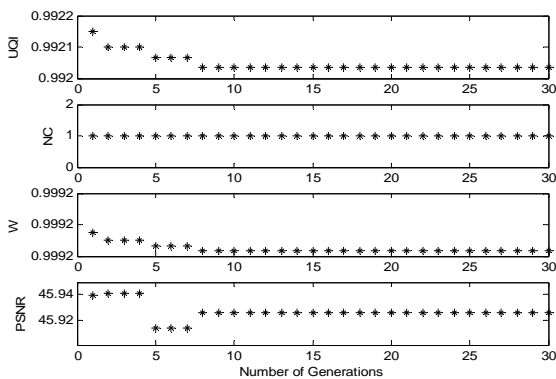

Fig.12 UQI , NC , W and $PSNR$ from GA optimization process of the Peppers image

Fig.13 Original "Lena" image

Fig.14 Watermarked "Lena" image using the proposed method

We first examine the robustness against JPEG compression. Tables 2–4 show the normalized correlations of the test images under JPEG compression with quality factor 30% to 90%. The watermark could be extracted from the JPEG compression image with quality factor as low as 30%. This demonstrates that the DMTGA is very robust to JPEG compression.

Next, we test the robustness with respected to SPIHT compression. The experiment results are shown in Table 5 to Table 7. In this case, the detector of the DMTGA method behaves significantly better than in the JPEG case. This could be explained by the fact that the image quality obtained by SPIHT is higher than that obtained by JPEG at the same compression ratio. Therefore, the watermark signal is better preserved by SPIHT compression.

Table 1 The results of parameters using GA optimization process from various image

Images	S_1	S_2	S_3	$PSNR$	NC
Lena	49.30	38.60	26.74	46.16	1.0
Baboon	47.88	38.59	27.91	46.46	1.0
Goldhill	47.65	37.76	23.26	46.70	1.0
Peppers	49.53	37.51	28.63	45.92	1.0

Table 2 Normalized correlation from JPEG compression of the Lena image

JPEG Quality factor (%)	Normalized correlation		
	[5]	[8]	DMTGA
30	0.1500	0.5391	0.9932
40	0.2300	0.7227	1.0000
50	0.2600	0.9023	1.0000
70	0.5700	0.9844	1.0000
90	1.0000	1.0000	1.0000

Table 3 Normalized correlation from JPEG compression of the Goldhill image

JPEG Quality factor (%)	Normalized correlation		
	[5]	[8]	DMTGA
30	0.2300	0.50	1.00
40	0.5200	0.74	1.00
50	0.7100	0.90	1.00
70	0.9300	1.00	1.00
90	1.0000	1.00	1.00

Table 4 Normalized correlation from JPEG compression of the Peppers image

JPEG Quality factor (%)	Normalized correlation		
	[5]	[8]	DMTGA
30	0.3400	0.52	0.99
40	0.5400	0.65	1.00
50	0.7000	0.81	1.00
70	0.9700	0.98	1.00
90	1.0000	1.00	1.00

Table 5 Normalized correlation from SPIHT compression of the Lena image

Bit rate (Bit per pixel)	Normalized correlation		
	[5]	[8]	DMTGA
0.3	0.2100	0.5703	0.9627
0.4	0.4100	0.7813	0.9931
0.5	0.8500	0.9102	1.0000
0.6	0.8300	0.9453	1.0000
0.7	0.8500	0.9570	1.0000

Table 6 Normalized correlation from SPIHT compression of the Goldhill image

Bit rate (Bit per pixel)	Normalized correlation		
	[5]	[8]	DMTGA
0.3	-0.0600	0.48	0.93
0.4	0.0200	0.58	0.96
0.5	0.2300	0.62	0.96
0.6	0.2700	0.74	0.99
0.7	0.3500	0.95	0.99

Table 7 Normalized correlation from SPIHT compression of the Peppers image

Bit rate (Bit per pixel)	Normalized correlation		
	[5]	[8]	DMTGA
0.3	0.3600	0.54	0.96
0.4	0.6600	0.67	0.99
0.5	0.6500	0.85	1.00
0.6	0.7100	0.92	1.00
0.7	0.8500	0.92	1.00

Finally, we perform image manipulations to the watermarked image such as median filtering, Gaussian filtering and image rotations. The comparison results are listed in Table 8 to Table 10. Through these tables, we can see that the DMTGA method is very robust to various attacks and yields significant more robust watermark than the methods in [5] and [8] do.

Table 8 Normalized correlation from signal processing attacks of the Lena image

Attack	Normalized correlation		
	[5]	[8]	DMTGA
2x2 Median filtering	0.3800	0.4648	0.7035
3x3 Median filtering	0.5100	0.6445	0.7960
4x4 Median filtering	0.2300	0.4492	0.5942
Gaussian filtering	0.6400	0.6680	0.9013
Rotation 0.5	0.2900	0.4570	0.6128
Rotation 1.0	0.2400	0.4219	0.4277
Rotation -0.5	0.2300	0.4609	0.6454
Rotation -1.0	0.1600	0.4180	0.5951

Table 9 Normalized correlation from signal processing attacks of the Goldhill image

Attack	Normalized correlation		
	[5]	[8]	DMTGA
2x2 Median filtering	0.3500	0.42	0.71
3x3 Median filtering	0.5600	0.51	0.96
4x4 Median filtering	0.2400	0.42	0.64
Gaussian filtering	0.5600	0.58	0.84
Rotation 0.5	0.2400	0.44	0.66
Rotation 1.0	0.1500	0.43	0.60
Rotation -0.5	0.2700	0.42	0.62
Rotation -1.0	0.1400	0.43	0.60

Table 10 Normalized correlation from signal processing attacks of the Peppers image

Attack	Normalized correlation		
	[5]	[8]	DMTGA
2x2 Median filtering	0.4600	0.49	0.65
3x3 Median filtering	0.7100	0.70	0.98
4x4 Median filtering	0.2500	0.47	0.63
Gaussian filtering	0.7400	0.81	0.89
Rotation 0.5	0.3000	0.44	0.64
Rotation 1.0	0.1700	0.43	0.61
Rotation -0.5	0.2500	0.45	0.61
Rotation -1.0	0.1600	0.42	0.65

5 CONCLUSION

This paper proposed a digital image watermarking algorithm in the multiwavelet transform domain. The embedding technique is based on the quantization index modulation technique and the watermark extraction algorithm does not need the original image in extraction process. In our optimization process, we use genetic algorithms searching for optimal parameters which are three quantization steps. These parameters are optimally varied to achieve the most suitable watermarked image for each given image. The experimental results demonstrate that the watermark from the proposed algorithm is robust to common attacks such as median filtering, Gaussian filtering, image

rotation and lossy compression. Further research can be concentrated on the development of our proposed method by using the characteristics of the human visual system.

Acknowledgement

References:

[1] F. Hartung and M. Kutter, "Multimedia Watermarking Techniques," Proc. IEEE, vol. 87, no. 7, pp. 1079-1107, July 1999.

[2] B. Chen and G. Wornell, "Quantization Index Modulation: A Class of Provably Good Methods for Digital Watermarking and Information Embedding," *IEEE Trans. on Information Theory*, vol. 47 no. 4, pp. 1423–1443, May 2001.

[3] S. Wu, J. Huang, D. Huang and Y. Q. Shi, "Efficiently Self-Synchronized Audio Watermarking for Assured Audio Data Transmission," *IEEE Trans. on Broadcasting*, vol. 51. no. 1, pp. 69–76, March 2005.

[4] S. Xiong, J. Zhou, K. He and F. Lang, "A Multipurpose Image Watermarking Method Based on Adaptive Quantization of Wavelet Coefficients," *Proc. Computer and Computational Sciences*, vol. 1, pp. 294-297, June 2006.

[5] S. H. Wang, and Y. P. Lin, "Wavelet Tree Quantization for Copyright Protection Watermarking," *IEEE Trans. on Image Processing*, vol. 13, no. 2, pp.154-165, 2004.

[6] L. Ghouti, A. Bouridane, M. K. Ibrahim and S. Boussakta, "Digital image watermarking using balanced multiwavelets," *IEEE Trans. on Signal Processing*, vol. 54, pp. 1519-1536, Apr. 2006.

[7] P. Kumsawat, K. Attakitmongcol, A. Srikaew, "Comparative Performance of Multiwavelet-Based Image Watermarking Schemes," *WSEAS Trans. on Systems*, vol. 5, pp. 1041-1047, May 2006.

[8] ——, "A Robust Image Watermarking Scheme Using Multiwavelet Tree," *Proc. World Congress on Engineering*, vol. 1, pp. 612-617, July 2007.

[9] M. Shinohara, F. Motoyoshi, O. Uchida and S. Nakanishi, "Wavelet-Based Robust Digital Watermarking Considering Human Visual System," *WSEAS Trans. on Signal Processing*, vol. 3, pp. 185-190, Feb. 2007.

[10] C. H. Huang and J. L. Wu, "A Watermark Optimization Technique Based on Genetic Algorithms," *Proc. SPIE Visual Communications and Image Processing*, vol. 3971, pp. 516-523, Feb. 2000.

[11] C. S. Shieh, H. C. Huang, F. H. Wang, J. S. Pan, "Genetic Watermarking Based on Transform-Domain Techniques," *Pattern Recognition*, vol. 37, no. 3, pp. 555-565, 2004.

[12] P. Kumsawat, K. Attakitmongcol and A. Srikaew, "A New Approach for Optimization in Image Watermarking by Using Genetic Algorithms," *IEEE Trans. on Signal Processing*, vol.53, pp. 4707-4719, Dec. 2005.

[13] F. Y. Shih and Y. T. Wu, "Enhancement of Image Watermark Retrieval Based on Genetic Algorithms," J. Vis. Commun. Image R, vol. 16, pp. 115-133, April 2005.

[14] N. Zhong, Z. He, J. Kuang and Z. Zhuo, "An Optimal Wavelet-based Image Watermarking via Genetic Algorithm," *Proc. Natural Computation*, vol. 3, pp. 103-107, Aug. 2007.

[15] N. Sriyingyong, and K. Attakitmongcol, "Wavelet-based Audio Watermarking Using Adaptive Tabu Search," Proc. IEEE Int. Symp. Wireless Pervasive Computing, vol.1, pp. 1-5, Jan. 2006.

[16] X. Y. Wang, H. Y. Yang and C. Y. Cui, "An SVM-Based Robust Digital Image Watermarking Against Desynchronization Attacks," Signal Processing, vol. 88, No. 9, pp. 2193-2205, Sept. 2008.

[17] Y. Zhang, "Blind Watermark Algorithm Based on HVS and RBF Neural Network in DWT Domain," *WSEAS Trans. on Computers*, vol. 8, pp. 174-183, Jan. 2009.

[18] S. J. Geronimo, D. P. Hardin and P. R. Massopust, "Fractal Functions and Wavelet Expansions Based on Several Scaling Functions," J. Approx. Theory, vol. 78, pp. 373–401, Sep. 1994.

[19] K. Attakitmongcol, D. P. Hardin and D. M. Wilkes, "Multiwavelet Prefilters II: Optimal Orthogonal Prefilters", *IEEE Trans. on Image Processing,* vol. 10, pp. 1476–1487, Oct.2001.

[20] J. H. Holland, *Adaptation in Natural and Artificial Systems*, Ann Arbor, MI: Univ. of Michigan Press, 1975.

[21] Z. Wang and A. C. Bovik, "A Universal Image Quality Index,"*IEEE Signal Processing Letters,* vol. 9, pp. 81-84, Mar. 2002.